iJRASET
International Journal For Research in Applied Science and Engineering Technology

INTERNATIONAL JOURNAL FOR RESEARCH
IN APPLIED SCIENCE & ENGINEERING TECHNOLOGY

Volume: 4 Issue: VI Month of publication: June 2016

DOI:

Volume 4 Issue VI, June 2016
ISSN: 2321-9653
International Journal for Research in Applied Science & Engineering Technology (IJRASET)

FEA analysis of notched adherent joint between metal and composite object using ANSYS CZM technique

Pravesh Kumar Soni[1], Mr. Hari Ram Chandrakar[2]
[1]*M.E. Final Year Student,* [2]*Assistant Professor,*
Mechanical Engineering, Shankaracharya Technical Campus, Shri Shankaracharya Group of Institutions (FET),
Junuani, Bhilai, Chattishgarh.

Abstract— Traditionally in engineering, structural joining has been synonymous to riveting, bolting and other purely mechanical fastening together with welding or soldering in the case of metallic construction materials. Up until the introduction of the polymeric adhesives around the time of the Second World War these were the only means of joining available but with the increased use of plastics, and more importantly fibre reinforced composite materials, the use of adhesive joining has increased rapidly and is today found in numerous applications with different material configurations. The reason for the increased use of adhesive joining is that it can provide a number of structural and economic advantages over more traditional methods of joining, of course assuming that the joint is properly designed. One of the most important features to keep in mind during the initial joint design is that adhesive joints are very strong in shear, but unfortunately are very vulnerable to normal stresses (in the context of adhesives commonly referred to as peel stresses).
Keywords— Asymmetric gear, Stress relieving feature, Circular hole, Elliptical hole, Von-Misses stress.

I. INTRODUCTION

Traditionally in engineering, structural joining has been synonymous to riveting, bolting and other purely mechanical fastening together with welding or soldering in the case of metallic construction materials. Up until the introduction of the polymeric adhesives around the time of the Second World War these were the only means of joining available but with the increased use of plastics, and more importantly fibre reinforced composite materials, the use of adhesive joining has increased rapidly and is today found in numerous applications with different material-configurations [3].

The reason for the increased use of adhesive joining is that it can provide a number of structural and economic advantages over more traditional methods of joining, of course assuming that the joint is properly designed. One of the most important features to keep in mind during the initial joint design is that adhesive joints are very strong in shear, but unfortunately are very vulnerable to normal stresses (in the context of adhesives commonly referred to as peel stresses). Provided that the joint is loaded in its favourable direction, some of the advantages are [4]:

- High strength to weight ratio
- Stresses distributed evenly over the joint width
- No drilled holes needed
- Weight and material cost savings
- Improved aerodynamic surface design
- Superior fatigue resistance
- Outstanding electrical and thermal insulation

As with any other technology, there are also limitations to consider when using adhesives in engineering. Elevated temperatures and high humidity can result in negative effects on the strength of some types of adhesives, especially when under continuous stress, and as with other polymeric materials, creep effects must be considered. Even though manufacturing procedures such as drilling, machining and riveting can be avoided when using adhesive fastening, this is replaced with a need for careful surface preparation prior to bonding, especially when using metal adherents.

Volume 4 Issue VI, June 2016
ISSN: 2321-9653
International Journal for Research in Applied Science & Engineering Technology (IJRASET)

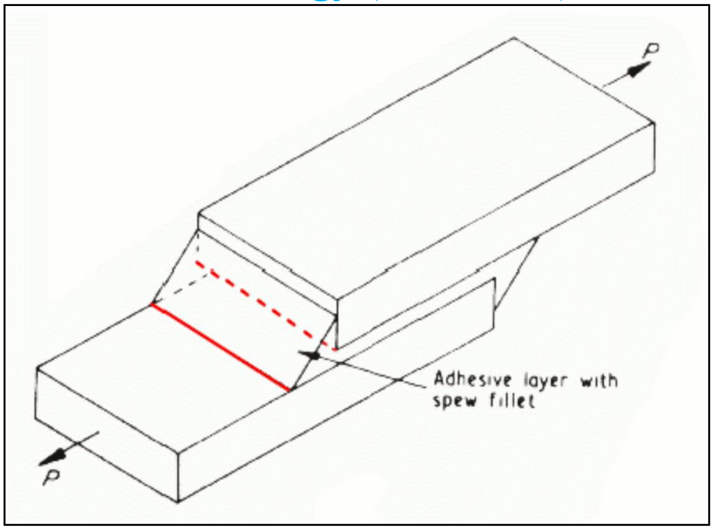

Figure2: Overview of a loaded SLJ with and without an adhesive spew fillet. Areas sensitive to crack initiation are marked in red.

In the typical case of an axially loaded DLJ the principal stresses in the adhesive layer are considerably higher at the ends of the adherents, both in shear and peel. This comes as a result of elasticity effects in the adherents and is seen in all types of adhesive joints. The result is that an adhesive joint when failing tends to crack open in one end and then peel open until completely parted. The magnitude of the stress concentrations is dependent of numerous factors such as adherent material and geometry as well as the physical properties of the adhesive. The level of the shear stress along the overlap length with both adherents made of carbon fiber reinforced plastic (CFRP, or commonly carbon fibre composite) is presented in Figure3 [5]

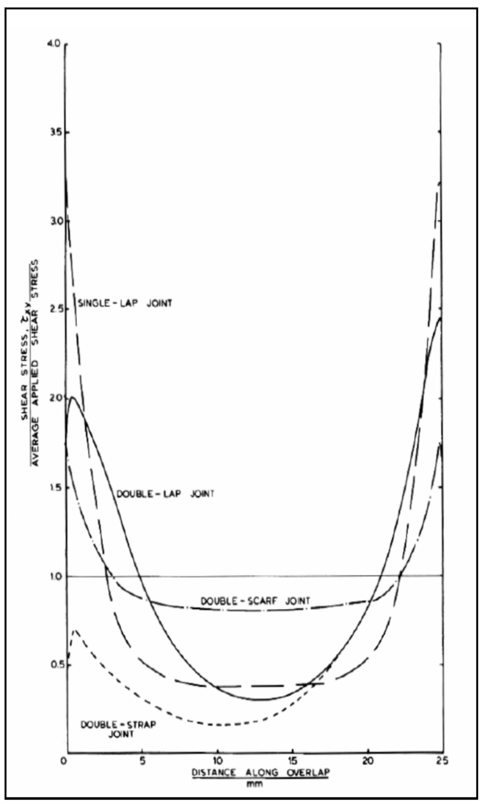

Figure 3: Adhesive shear stress distribution along the over-lap length of four different joint types with CFRP adherents

Volume 4 Issue VI, June 2016
ISSN: 2321-9653
International Journal for Research in Applied Science & Engineering Technology (IJRASET)

II. ANALYTICAL METHOD

When it comes to determining the stresses in a specific joint configuration, today numerical FE-methods are used almost exclusively. Over the years however, extensive work has been done on deriving analytical methods for describing the behavior of adhesive joints – a process that still continues. The foundations were laid out with the work of Volkersen in 1938 [6], where he derives a closed form mathematical solution for a simple case with tensional loaded adherents and an adhesive loaded only in shear

A. Volkersen's Shear Lag Analysis

The basic stress distribution given by equation $\tau = P/bl$ assumes the adherents to be rigid and the adhesive to deform only in shear. The tensile stress in the upper adherent will decrease linearly to zero from point A to point B. The converse is true for the lower adherent. Therefore the shear stress in the adhesive bond is constant, as shown in Figure 4. Note how the parallelograms are uniformly sheared. However, if the adherents are allowed to deform elastically, the adhesive shear stress distribution is dramatically different as shown in figure 4. For the upper adherent, the tensile stress is at a maximum at A and falls to zero at B, but not linearly. The converse is true for the lower adherent. Because the stress is at a maximum at A, the tensile strain at A is larger than at B and is reduced along the length of the bond line. This causes the parallelograms in figure 4 to become distorted as shown in figure 4. This distortion results in a non-uniform shear stress distribution along the adhesive/ adherent interface with peak stresses at the ends of the joint

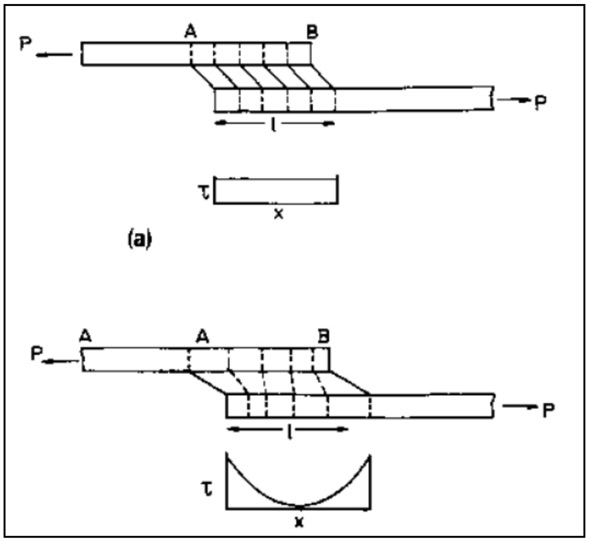

Figure 4: Deformation of a sinle lap joint (SLJ) with rigid adherents and elastic adherents.

V.O. Volkersen studied this phenomenon, termed differential shear, and in 1938 presented his shear lag analysis. In this analysis he assumed that the adhesive deforms only in shear, the adherents deform only in tension, and both the adhesive and adherents are linearly elastic. The adhesive shear stress distribution is given as:

$$\tau = \frac{\omega}{2}\frac{\cosh \omega X}{\sin\frac{\omega}{2}} + \left(\frac{\psi - 1}{\psi + 1}\right)\frac{\omega}{2}\frac{\sinh \omega X}{\cosh\frac{\omega}{2}} \quad (1)$$

Where,

$$\omega^2 = (1 + \psi)\,\phi \quad (2)$$

$$\psi = \frac{t_1}{t_2} \quad (3)$$

$$\phi = \frac{Gl^2}{Et_1 t_2} \quad (4)$$

$$X = \frac{x}{l} \quad (5)$$

In the above equations, t is the thickness, G is the adhesive shear modulus, E is the Young's modulus of the adherents and l is the

Volume 4 Issue VI, June 2016
ISSN: 2321-9653

length of the overlap. Subscripts 1, 2 and 3 are the two adherents and adhesive layer respectively.

While this method provides a classical elastic solution to the adhesive shear stress distribution in a single lap joint, it is not supported by experimental results. Volkersen did not take into account two important factors in his shear lag analysis. First, in a single-lap joint, the directions of the two forces are not collinear. Rather, the line of action of the load path is eccentric. These results in a bending moment applied to the joint as well as the in-plane tension. This eccentricity also gives rise to transverse normal or peeling stresses, which play a significant role in the mode of failure of the joint. Second, because the adherents bend, the joint rotates and the joint displacements are no longer proportional to the applied load. If this angel of rotation is large, the problem becomes geometrically nonlinear.

B. Goland and Reissner

In the 1940's, Goland and Reissner [7] improved Volkersen's analysis by including the deflection of the joint due to the bending moment and the peel stresses. Their stress analysis was divided into two parts. The first part involved determining the loads at the edges of the joint. The second part dealt with determining the stresses in the joint due to the applied load. Their assumptions were the following:

The normal stress parallel to the layer in the adhesive is neglected

All other normal stresses in the adhesive do not vary across the thickness

The problem is one of plane strain

By using strain energy methods and the above assumptions, they derived the overall strain energy in the joint. By minimizing the strain energy equation, the correct stress distribution, which satisfies equilibrium and the boundary conditions, was established for two limiting cases.

The first case assumes that the adhesive layer is very thin compared to the adherents and that all flexibility is due to the adherents. This case is also valid for relatively thick adhesive layers whose material properties are of the same order of magnitude as the adherents. The limiting values are:

$$\frac{t_3\,E_1}{t_1\,E_3} \leq 0.1 \;\; and \;\; \frac{t_3\,G_1}{t_1\,G_3} \leq 0.1 \qquad (6)$$

The second case assumes that the adhesive layer is relatively thick compared to the adherents and that all flexibility is due to the adhesive. The limiting values are:

$$\frac{t_1\,E_3}{t_3\,E_1} \leq 0.1 \;\; and \;\; \frac{t_1\,G_3}{t_3\,G_1} \leq 0.1 \qquad (7)$$

Most practical joints fall outside the bounds of case 2. Limitations of this theory include the inability to control the boundary and continuity conditions of the adhesive layer at the edges of the overlap. Because of this, the stress fields in the adhesive maintain global equilibrium, but not point equilibrium. This method is therefore accurate enough to determine the stress distributions in a global sense, but does not capture the local stress behavior in the adhesive. The shear stress distribution of Goland and Reissner is given by:

$$\tau_0 = \left(-\frac{1}{8}\right)\left(\frac{pt_1}{c}\right)\left[\frac{\beta c}{t_1}(1+3k)\frac{\cosh\left(\frac{\beta c x}{t_1 c}\right)}{\sinh\left(\frac{\beta c}{t_1}\right)} + 3(1-k)\right] \qquad (8)$$

Where,

$$\beta^2 = 8\frac{G_3}{E_1}\frac{t_1}{t_3} \qquad (9)$$

The transverse or peel stress distribution is given by:

$$\sigma_0 = \frac{pt^2}{c^2 R^3}\left[\begin{array}{c}\left(R_2\lambda^2\frac{K}{2} - \lambda K' \cosh\lambda\cos\lambda\right)\cosh\frac{\lambda x}{c}\cos\frac{\lambda x}{c} + \\ \left(R_1\lambda^2\frac{K}{2} - \lambda K' \sinh\lambda\sin\lambda\right)\sinh\frac{\lambda x}{c}\sin\frac{\lambda x}{c}\end{array}\right] \qquad (10)$$

Where,

$$\lambda = \gamma\frac{c}{t_1} \qquad (11)$$

$$\gamma^4 = 6\frac{E_3}{E_1}\frac{t_1}{t_3} \quad (12)$$

$$K' = K\frac{c}{t_1}\left[3(1-\nu^2)\frac{p}{E_1}\right]^{\frac{1}{2}} \quad (13)$$

$$c = \frac{l}{2} \quad (14)$$

$$R_1 = \cosh\lambda\sin\lambda + \sinh\lambda\cos\lambda \quad (14)$$

$$R_2 = \sinh\lambda\cos\lambda - \cosh\lambda\sin\lambda \quad (15)$$

III. CZM IN ANSYS

Fracture or delamination along an interface between phases plays a major role in limiting the toughness and the ductility of the multi-phase materials, such as matrix-matrix composites and laminated composite structure. This has motivated considerable research on the failure of the interfaces. Interface delamination can be modeled by traditional fracture mechanics methods such as the nodal release technique. Alternatively, you can use techniques that directly introduce fracture mechanism by adopting softening relationships between tractions and the separations, which in turn introduce a critical fracture energy that is also the energy required to break apart the interface surfaces. This technique is called the cohesive zone model. The interface surfaces of the materials can be represented by a special set of interface elements or contact elements, and a cohesive zone model can be used to characterize the constitutive behaviour of the interface.

IV. ABOUT TED AND IMPLEMENTATION OF CZM TECHNIQUE IN NON-LINEAR ANALYSIS OF TED

In a rocket engine turbines are used for the LOX and LH2 fuel supply pump systems. In the Hydrogen Turbo-Pump (TPH), high pressure gaseous hydrogen (GH2) provides the power through a turbine connected to the pump drive shaft. After passing the turbine, the GH2 is passed through the Turbine Exhaust Duct (TED) in which it is divided into a main flow to power the Oxygen Turbo-Pump (TPO) and a secondary by-pass that can be passed on directly to the combustion chamber. In this thesis TED design data has been adopted from The Vinci Engine Project and the TED which has been used in the Vinci Engine has been designed by Volvo Aero Corporation [12][14].

Vinci LH2 turbine data [12][14].

- Number of stages 1
- Nominal speed 91,000 rpm (max 102,000)
- Nominal power output 2500 kW (max 3700 kW)
- Mean gas diameter 120 mm
- Mass flow 4.9 kg/s
- Turbine inlet pressure 180 Bar (max 232 Bar)
- Turbine inlet temperature 245 K (Max 325 K)
- Pressure ratio 2:1

The TED operates under very demanding conditions with cryogenic temperatures, high inter-nal pressure, external structural loads and a pure hydrogen environment. Typically during an engine run cycle, the temperature inside the TED varies between room temperature and -140°C and the internal pressures reaches as high as 10 MPa. Naturally this is very stressing on the component material and the present TED is a robustly designed in cast Inconel 718, a nickel-based “super alloy”.

For this project, a CZM approach has been chosen for analysing the adhesive interfaces using the CAE software package ANSYS 11.0. Using CZM to analyse adhesive contact is available in ANSYS as a special case of regular contact analysis where a specially defined CZM mate-rial is used on the contact surfaces. The specific cohesive zone model implemented by AN-SYS is based on the methods described by Alfano and Crisfield [17] and uses a mixed mode description to handle the different susceptibilities to fracture in mode I (normal) and mode II (shear) loading.

Before a two dimensional transient couple field analysis has been performed for a TED design, a transient test has been done on a simple metal-composite adhesive bonding for validation of the CZM technique of ANSYS.

Volume 4 Issue VI, June 2016
ISSN: 2321-9653
International Journal for Research in Applied Science & Engineering Technology (IJRASET)

V. ANALYTICAL VALIDATION OF ANSYS CZM

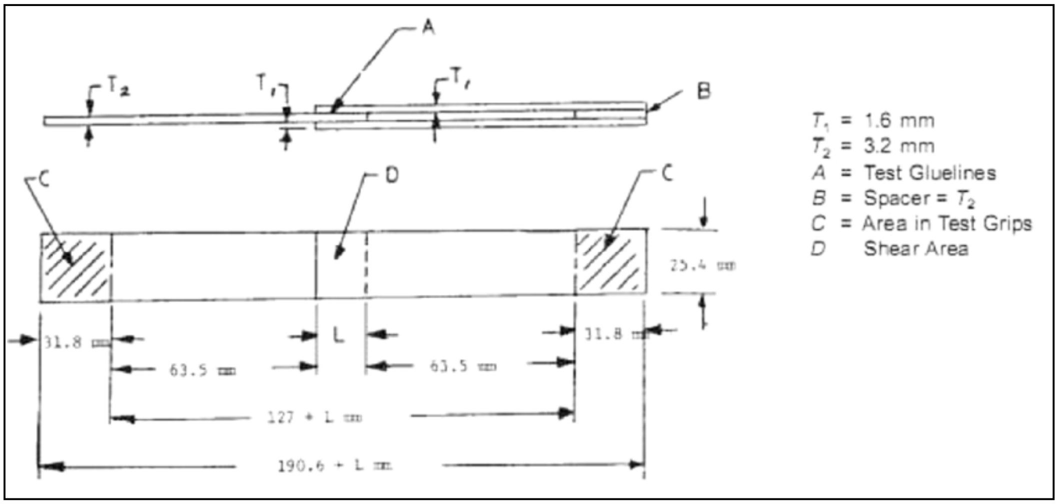

Figure 5: Double lap joint test specimen according to standard ASTM D3528-96

To validate FEA model of TED analysis the above mentioned test has been simulated in ANSYS using its CZM technique. The specimen configuration which has been used for this simulation has been mentioned below.

The symmetric geometry of a DLJ test specimen makes it very suitable for modelling using symmetry conditions and simplified stress assumptions. To take full advantage of this, the model used for the majority of the analyses is a 2D plane strain model with a longitudinal symmetry boundary condition in the mid-plane of the centre adherent (Figure 4.1). The di-mensions are essentially those defined in the ASTM standard for DLJ tests, ASTM D3528-96 (See Figure 3.2), with an alteration of the adherent base thickness (T1 and T2) from 1.6 mm to 2 mm due to the thickness of the titanium plates used in the construction of the specimens.

The model geometry was meshed in ANSYS 11.0 with PLANE182, a 4-node structural solid element, and a base element size of 0.5 mm. The area around the adhesive zone was further refined to a mesh size of approximately 0.2 mm and then meshed with contact elements to simulate the adhesive layer (see Figure 3.3). Even though the adhesive in fact has a thickness of 0.2 mm it is in the FE-model defined as a zero-thickness cohesive zone, with 2-node CONTA171 contact elements on one adherent and corresponding TARGE169 target elements on the other. The physical behaviour of the adhesive layer thickness must therefore be cor-rected through the contact penalty stiffness parameters Kn and Kt.

Once the model was set up and meshed, the boundary conditions (apart from symmetry) were simply applied as a zero displacement on the CFRP adherent end face and a prescribed displacement of 0.7-1 mm to the other end face. This is of course a simplification to the real world scenario with hydraulic grips holding the specimen, but was initially deemed sufficient since the main point of interest was the adhesive area in between. Figures below represent the geometry of the specimen.

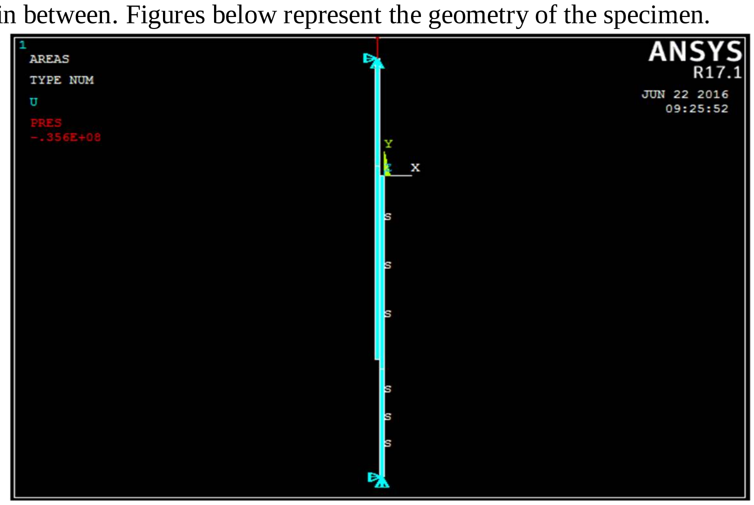

Figure 6: Symmetric model of Double lap joint test specimen

Volume 4 Issue VI, June 2016
ISSN: 2321-9653

Now above model has been meshed using a quadrilateral element named PLANE182 and the cohesive boned has been FEA modeled using contact elements CONTA171 and TARGE169. The CONTA171 element is not exclusively a cohesive zone element and can be used to simulate a variety of contact conditions of which bonded contact with CZM materials is a special case. It is a 2-node element that is overlaid on an existing solid, shell or beam element face and share nodes and geometry with these "parental elements" (see Figure 4.4). To define the cohesive debonding behavior in ANSYS, first a CZM material has to be defined through the TB command with CZM label. This material data table contains the values of the maximum stresses, fracture energies and the artificial damping coefficient of the material. Secondly the selected interfaces are meshed with contact and target elements using the ESURF command and with the CZM material activated. The bonding properties are set through the element KEYOPTs and finally the penalty stiffnesses can be adjusted through setting the REAL constants related to the contact elements. Target elements are meshed with ESURF in the same manner as the contact elements but do not require any additional settings.
Figure below shows the meshed view of the specimen in enlarged view.
After successful completion of mashing, proper Boundary Conditions have been implemented. One end of the specimen has been hold with its all degree of freedom restricted. Other end of the cohesive joint has been given a predefined displacement of 0.8 mm along Y-axis and it degree of freedom along X-axis has been made zero i.e restricted.
In this test simulation of DLJ specimen adhesive joint has been made between an isotropic material Titanium-Aluminum alloy Ti 6Al-4V and a composite material Carbon Fiber Reinforced Plastic (CFRP). Material properties used for the Ti 6Al-4V (Which is also known as EA-9394) and the CFRP have been mentioned below.

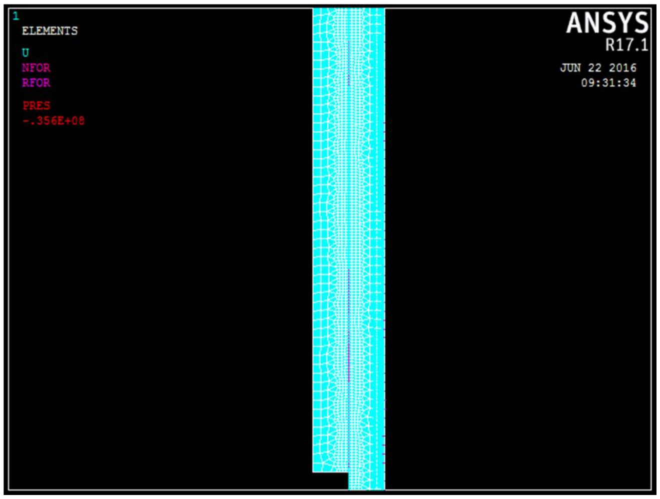

Figure 7: Enlarged meshed view of the specimen model.

Table 1: Material Properties of DLJ specimen components for Structural analysis [12][14].

Parameters	CRFP (Composite)	EA 9394 (Isotropic)	Units
Elastic Modulus (Ex / Ey / Ez)	10.1/52.9/52.9	114	GPa
Poisson's Ratio (vxy /vyz/vzx)	0.056 / 0.317 / 0.056	0.3	-
Shear Modulus (Gxy/Gyz/Gzx)	3.69 / 20.1 / 3.69	-	GPa

Result from the above mentioned simulation which has been done by ANSYS CZM technique through an APDL program has been validated with the result value derived analytically using previously mentioned Volkersen's Shear Lag theory and Goland and Reissner thory. The FEA results have been mentioned below.

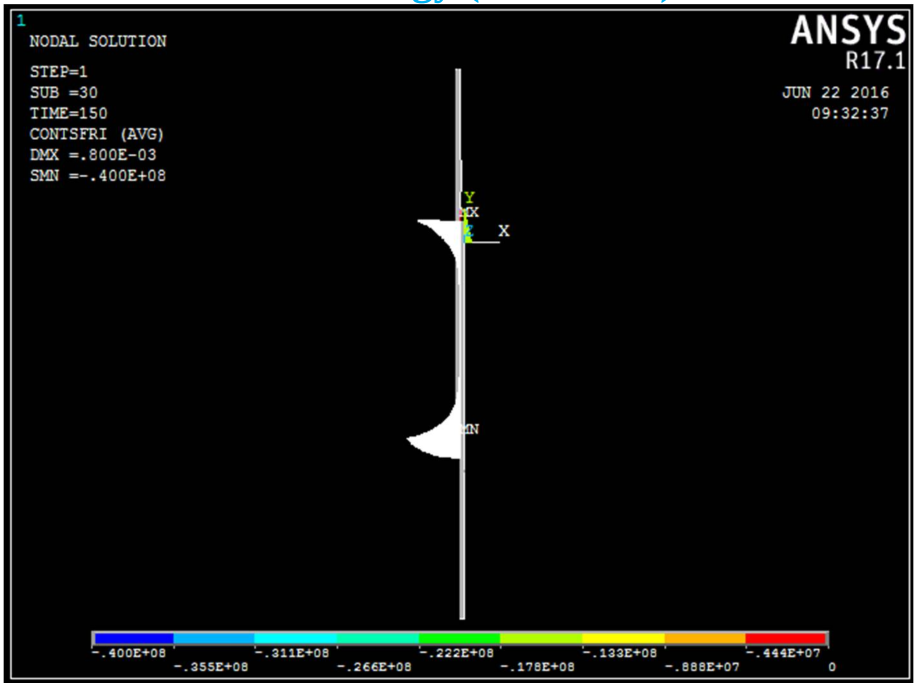

Figure 8: Adhesive shear stress at uy = 0.8 mm for the same test specimen of ref [12]&[14] as per this work

VI. 2D AXISYMMETRIC TED ANALYSIS

Here in this section a TED joint has been analysed using ANSYS CZM and has been validated with previous work of reference [12] and [14]. The geometrical details and material properties have been taken from the reference [12] and [14].

Geometry

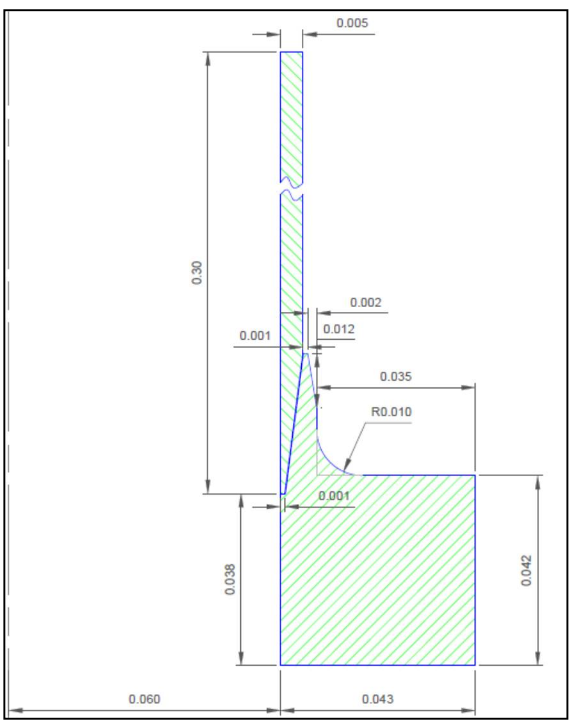

Figure 10: Basic measurements and BC's of modified (tapered) adhesive joint configuration

Material Properties:

Volume 4 Issue VI, June 2016
ISSN: 2321-9653
International Journal for Research in Applied Science & Engineering Technology (IJRASET)

Table 2: Material Properties of DLJ TED for Couple-field Transient analysis [12][14].

Parameters	CRFP (Composite)	EA 9394 (Isotropic) (Ti 6Al-4V)	Units
Elastic Modulus ($E_x / E_y / E_z$)	10.1/52.9/52.9	114	GPa
Poisson's Ratio (ν_{xy} /ν_{yz}/ν_{zx})	0.056 / 0.317 / 0.056	0.3	-
Shear Modulus (G_{xy}/G_{yz}/G_{zx})	3.69 / 20.1 / 3.69	-	GPa
CTE (α_{xx}/ α_{yy}/ α_{zz})	56.1×10^{-6} /3.8×10^{-6} /3.8×10^{-6}	69×10^{-6}	K^{-1}
Spec. Heat Capacity (C_p)	900	1340	J/kgK
Density (ρ)	1528	1150	Kg/m^3
Thermal Conductivity (k_{xx}/k_{yy}/ k_{zz})	0.78/5.54/5.54	0.24	W/ mK
Max contact stress (σ_{max}/ τ_{max})	-	44.5/40	GPa
Critical Fracture Energy (G_{Ic}/G_{IIc})	-	425/2000	J/m^2
Contact Stiffness (K_n/K_t)	-	2×10^{13}/1×10^{12}	N/m^2

As per the given dimensions the model has been generated in ANSYS through APDL Program. After creating a 2-dimensional model in ANSYS now the model has been meshed with PLANE223 element and adhesive connection has been created with element TARGE169 and CONTA172. Meshed view has been shown below.

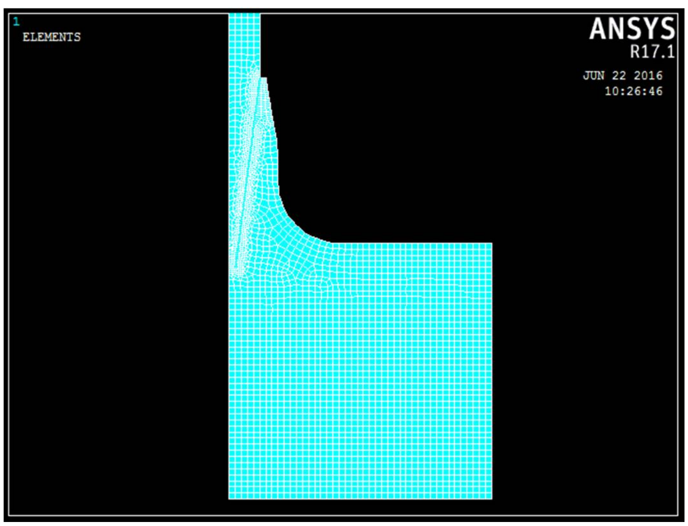

Figure 11: Meshed view of the 2D geometry.

Volume 4 Issue VI, June 2016
ISSN: 2321-9653

After the solution done, different results have been derived for study. Here following results have been derived.

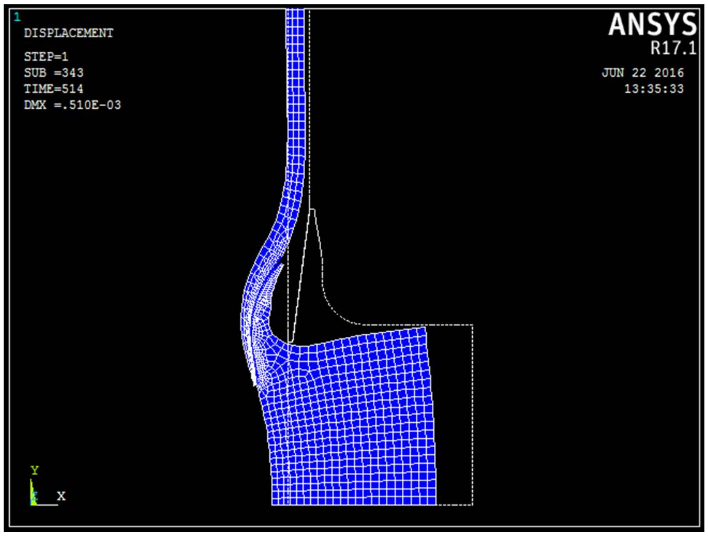

Figure 12: Deflection of the model under the structural and thermal loading.

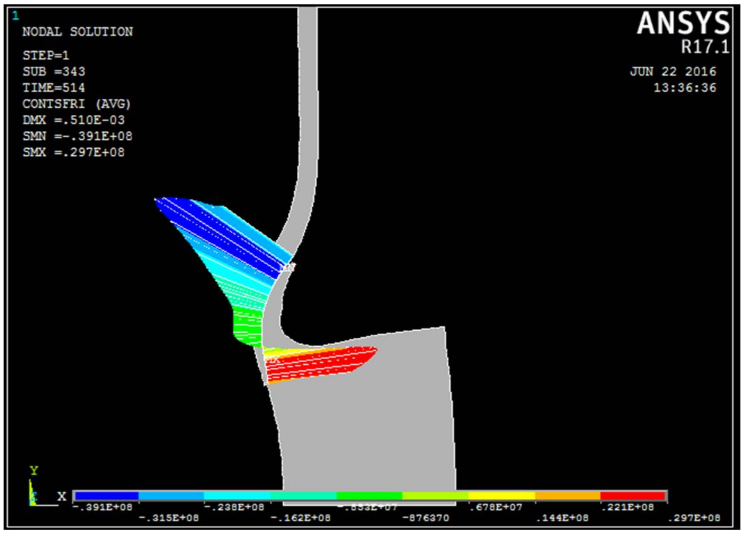

Figure 13: Contact frictional stress distribution under the structural and thermal load.

VII. FURTHER MODIFICATIONS IN TED GEOMETRY

In previous section shear stress analysis has been done on TED geometry with beveled edge adhesion surface. Concept of this type of adhesive geometry was incurred by Fros Fredrik Fors in his Phd thesis (Reference [14]). The beveled edge adhesive joint he called in his thesis as ‘Tapered Edge’ adhesive joint. Though he incurred or mentioned this conception in his thesis but did not analyze or simulate it in ANSYS. In the previous chapter of this work a simulation has been done on ‘Tapered Edge’ adhesive joint of TED using ANSYS CZM technique and results have been discussed in detail. In this chapter of this work analysis has been done on a modified edge TED adhesive joint and results of ‘Tapered Edge’ adhesive joint and ‘Modified Edge’ adhesive joint of TED has been compared.

In this modified geometry end configuration of the adhesive joint has been changed. Also the taper angle of the beveled part has been changed. In previous tapered joint of TED, the taper angle was 7.35° and the end configuration was straight type of length 0.001 m. But in the modified TED adhesive joint the taper angle has been changed to 3.69° and the end configuration has been also modified and has been shown in figure below.

As it has been mentioned earlier that when an adhesive joint is subjected to a system of loading there are two types of stress appeared on the adhesive surface and these are ‘Frictional Shear Stress’ and ‘Peal Stress’. With the configuration explained in chapter 5 there is little prevention against the peel stress but if the modified end configuration is used as explained in this chapter,

Volume 4 Issue VI, June 2016
ISSN: 2321-9653
International Journal for Research in Applied Science & Engineering Technology (IJRASET)

there will be a great prevention against the peel stress.

Now generating the modified configuration a simulation has been done in ANSYS using its CZM Technique to check whether this modification increase the friction shear stress or not.

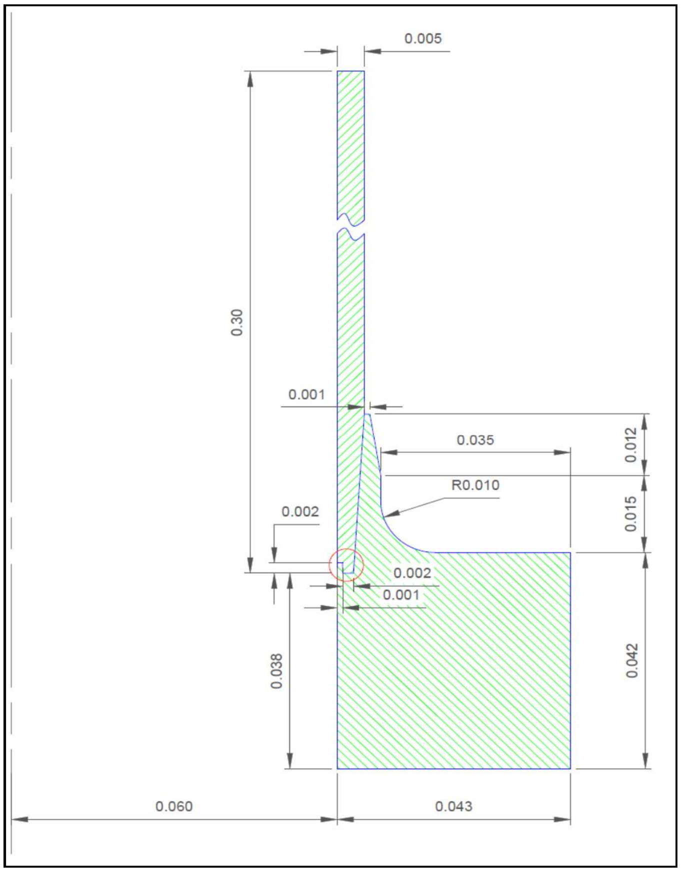

Fig. 15: Meshed Geometry of Modified configuration of TED adhesive joint generated in ANSYS

On completion of non-linear solution frictional shear stress of the adhesive line has been determined to check whether this modification in adhesive geometry increases the shear stress in comparison with the shear stress determined for the case of tattered joint as discussed in previous sections.

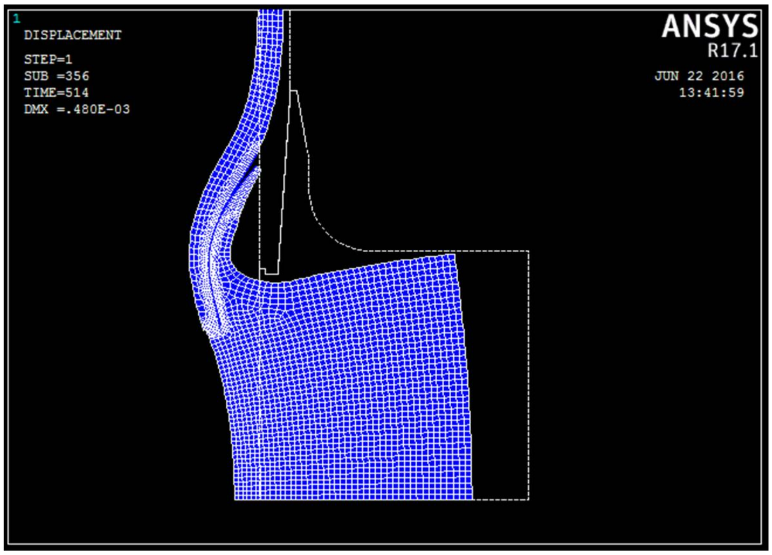

Figure 16: Deflection of the model under the structural and thermal loading.

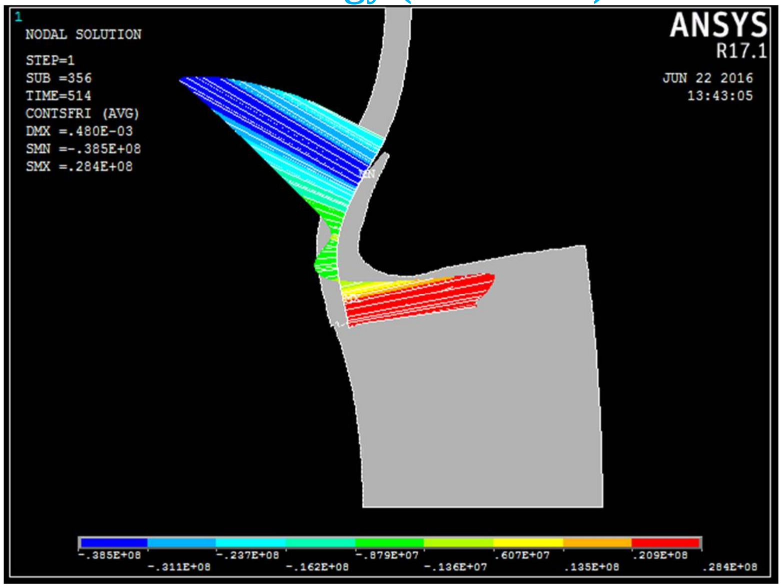

Figure 17: Contact frictional stress distribution under the structural and thermal load.

From the above results it is quite clear that the modification in adhesive joint configuration generates a frictional shear stress of 28.4 MPa along the adhesive layer. This value is not more than the frictional shear stress generated in the tapered configuration as discussed in previous sections, which is 29.9 MPa. Also the deflection occurred in the configuration mentioned in 5th chapter was 0.510 mm but the same loading system gives the defection in the modified geometry only 0.507 mm which is less that the defection occurred in the tapered adhesive joint configuration mentioned in previously.
Moreover, the stepped end configuration of the modified geometry as discussed in this chapter will prevent the adhesive configuration to be peeled out under a system of loading, which is advantageous.

VIII. CONCLUSIONS AND FUTURE SCOPE

It has already been discussed that, due to advancement of material science many composite materials have been created which having more strength than the conventional isotropic materials and at the same time much lighter in Wright than those conventional isotropic material. But with the evolvement of these composite materials a new challenge has been raised in-front of us. By conventional fastening methods like Riveting, Bolting and Welding it is nearly impossible to attach two components made of composite materials or one made of isotropic material and other of composite material. To counter this challenge a new fastening technology has been invented through rigorous R-n-D on adhesion technique. Through continuous research activities new types of adhesives have been created to fasten two components made of composite materials or one made of isotropic material and other of composite material. For example Haysol EA 9394, which is capable to fasten two components one made of composite materials and other made of metal. But these adhesives have a limitation to withstand a system of loading up to a definite level. Moreover, these adhesives are though highly capable to withstand frictional shear stress but very much prone to peel stress.
Therefore, it is very much necessary to design efficiently the adhesion surface edge so that resistance against the peel stress can be created without hampering the resistance capability of adhesives against the frictional shear stress. But it is not easy to do research with different edge configuration, because composite materials are very costly and also it is very difficult to do machining on the composite materials. So, to keep the research process cost effective and to make the end product economically viable, numerical process has to be adopted.
It may be concluded that Cohesive Zone Model approach of ANSYS, as discussed in previous chapters, is a powerful alternative when analyzing the complex process of adhesive debonding. The major benefit is that the entire process from crack initiation to complete debonding through elastic displacement and damage/softening of the adhesive is included in the model and can be handled in a single analysis. No crack-tip elements or similar is needed as in other LEFM-based methods and the location of the initiation of fracture, or debonding, is also determined by the FE model. CZM provides a clear failure criterion included in the cohesive law that makes it possible to analyze both partial and complete debonding.
As discussed earlier that when an adhesive joint is subjected to a system of loading there are two types of stress appeared on the

adhesive surface and these are 'Frictional Shear Stress' and 'Peal Stress'. With the configuration explained in chapter 5 there is little prevention against the peel stress but if the modified end configuration is used as explained in this chapter, there will be a great prevention against the peel stress.

Now generating the modified configuration a simulation has been done in ANSYS using its CZM Technique to check whether this modification increase the friction shear stress or not.

One of the disadvantages is that a CZM analysis requires material parameters specialized for the joint configuration in question, that typically are not available readily. Acquiring these parameters through testing is not particularly difficult, but the procedures, although mostly standardized by ASTM and ISO, still require resources and competence not available everywhere. As has been shown by this report, determining material parameters indirectly through e.g. tensile tests is a possible way to go, but must still be considered a secondary alternative to dedicated experimental testing. Another limitation to CZM worth mentioning is that the debonding only occurs along the plane defined by the cohesive zone elements. This is usually not an issue when modeling adhesive joints but can be bothersome when modeling composite adherents where the crack can advance into the layers of the composite.

As the future scope, it is worthy to mention that frictional stress of the adhesive joint may be increased by improving the design of a joint configuration. So by optimizing different design parameters of a joint configuration we can have minimum frictional shear stress for a minimum adhesive length. It is because if we keep the adhesive length minimum we will get minimum peel stress on the joint.

REFERENCES

[1] Gupta N. K., " Turbomachines for Cryogenic Engines", Proceedings of the 37th National & 4th International Conference on Fluid Mechanics and Fluid Power, Decenber 2010, IIT Madras.
[2] MATTSON D, LUNDSTRÖM R AND EMAN J, "Preliminary studies of typical stresses in composite to metal joints for aerospace applications," CR09-25, Swerea SICOMP, Piteå, 2009.
[3] BHOWMIK S, BENEDICTUS R, POULIS J A, BONIN H W AND BUI VT, "High-performance nanoadhesive bonding of titanium for aerospace and space application," International Journal of Adhesion & Adhesives, 2009, 29:259-267.
[4] TOMBLIN J S, YANG C, and Hartner P, "Investigation of Thick Bondline Adhesive Joints," DOT/FAA/AR-01/33, U.S. Department of Transportation, Washington, DC, 2001.
[5] ADAMS R D, Comyn J, and Wake W C, Structural Adhesive Joints in Engineering, 2nd ed. London, UK: Chapman & Hall, 1997.
[6] VOLKERSEN O, "Die Nietkraftverteilung in zugbeanspruchten Nietverbindungen mit konstanten Laschenquerschnitten," Luftfahrtsforschung, 1938, 15:41-47.
[7] GOLAND M AND REISSNER E, "The Stresses in Cemented Joints," Journal of Applied Mechanics, ASME, 1944; 66:A17-A27.
[8] TORSTENFELT B, Finite Elements - From the Early Beginning to the Very End, Preliminary ed. Linköping: Linköpings Univeristet, 2007.
[9] HUGHES T, The Finite Element Method: Linear Static and Dynamic Finite Element Analysis.: Dover Publications, 2000.
[10] HARRISON N L AND HARRISON W J, Journal of Adhesion, 1972; 3:195.
[11] WOOLEY G R AND CARVER D R, Journal of Aircraft, 1971; 8:8 17.
[12] JANS SON N, "Method for Estimation of Ultimate Strength of Adhesive Joints," VOLS: 10097121, Volvo Aero Corporation, Trolhättan, 2010.
[13] SCHMIDT P, "Computational Models of Adhesively Bonded Joints," Linköping University, Linköping, PhD Thesis 2007.
[14] Fredrik Fors, " Analysis of Metal to Composite Adhesive Joints in Space Applications Computational Models of Adhesively Bonded Joints," Linköping University, Linköping, PhD Thesis (LIU-IEI-TEK-A—10/00812—SE), 2010.
[15] IRWIN G R, "Analysis of stresses and strains near the end of a crack transversing a plate," Journal of Applied Mechanics, 1957; 24:361-366.
[16] ANDERSON T L, Fracture Mechanics - Fundamentals and Applications, 3rd ed. Boca Raton, FL: CRC Press, 2005.
[17] ALFANO G AND CRISFIELD M A, "Finite element interface models for the delamination analysis of laminated composites: mechanical and computational issues," International Journal for Numerical Methods in Engineering, 2001; 50:1701-1736.
[18] GUESS T R, REEDY E D, AND STAVIG M E, "Mechanical Properties of Hysol EA-9394 Structural Adhesive," SAND95-0229, Sandia National Laboratories, Albuquerque, NM, 1995.
[19] MATTSSON D, "Description of manufacturing and tests performed within the KOMET project," CR09-062, Swerea SICOMP, Piteå, 2009.
[20] "Standard test method for strength properties of double jap shear adhesive joints by tension loading," ASTM D3528-96 , 1996.
[21] GUNAWARDANA S, "Prediction of failure initiation of adhesevely bonded joints using mixed-mode fracture data," Wichita State University, Wichita, KS , M Sc Thesis 2003.
[22] EDGREN F, "Specification for application of composite to metal joint in engine environment," VOLS: 10075712, Volvo Aero Corporation, Trollhättan, 2009.
[23] MAGNUSSON K, "Material Specification: Forged Ti 6Al-4V," VOLS: 10086015, Volvo Aero Corporation, Trollhättan, 2009.
[24] LANGLOIS V, "Specification of selected external load cases for the partial structural justification of the exhaust casing of the Vinci hydrogen turbopump," Snecma Moteurs, Vernon, 2007.
[25] ANSYS INC. (2007) ANSYS 11.0 Release Documents. Chapter 9.1 Submodeling.
[26] KIM M-G, KANG S-G, KIM C-G, AND KONG C-W, "Tensile response of graphite/epoxy composites at low temperature," Composite Structures, 2006; 79:84-89.
[27] KIM M-G, KANG S-G, KIM C-G, AND KONG C-W, "Tensile properties of carbon fiber composites with different resin compositions at cryogenic temperatures," Advanced Composite Materials, 2010; 19:63-77.
[28] REED R P AND GOLDA M, "Cryogenic properties of unidirectional composites," Cryogenics, 1994; 34(1 1):909-928.
[29] GRAF N A, Schieleit G F and Briggs R, "Adhesive bonding characterization of composite joints for cryogenic usage," Lockheed Martin Space Systems, New

Volume 4 Issue VI, June 2016
ISSN: 2321-9653

Orleans, LA,.

[30] SHIMODA T, HE J, AND ASO S, "Study of cryogenic strength and fracture behaviour of adhesives for CFRP tanks of reusable launch vehicles," Memoirs of the Faculty of Engineering, Kyushu University, 2006; 66(1):55-70.

[31] BARTOSZYK A, JOHNSTON J, KAPERIELAN C, AND KUHN J, "Design/analysis of the JWST ISIM bonded joints for survivability at cryogenic temperatures," Proceedings of SPIE, 2005; 5868:1-10.

[32] KANG S-G, KIM M-G, AND KIM C-G, "Evaluation of cryogenic performance of adhesives using composite-aluminium double-lap joints," Composite Structures, 2007; 78:440-446.

[33] LUNDMARK P AND MATTSON D, "Mechanical testing of the composite-titanium joint studied in the KOMET project," CR1 0-017, Swerea SICOMP, Piteå, 2010.

[34] ANDRÉ A, "KOMET project results from FE models - cohesive modelling," Swerea SICOMP, Gothenburg, Presentation 2009.

[35] FUTRON CORPORATION, "Space transportation costs: Trends in price per pound to orbit 1999-2000," Bethesda, MD, 2002.

[36] AZARI A, PAPINI M, SCHROEDER J A, AND SPELT J K, "Fatigue theshold behavior of adhesive joints," International Journal of Adhesion & Adhesives, 2009; 30:145-159.

[37] MENEGHETTI G, QUARESIMIN M AND RICOTTA M, "Influence of the interface ply orientation on the fatigue behaviour of bonded joints in composite materials," International Journal of Fatigue, 2010; 32:82-93.

[38] ABDEL WAHAB M M, HILMY I, ASHCROFT I A, AND CROCROMBE A D, "Evaluation of fatigue damage in adhesive bonding: Part 2: Single lap joint," Journal of Adhesion Science and Technology, 2010; 24:325-345.

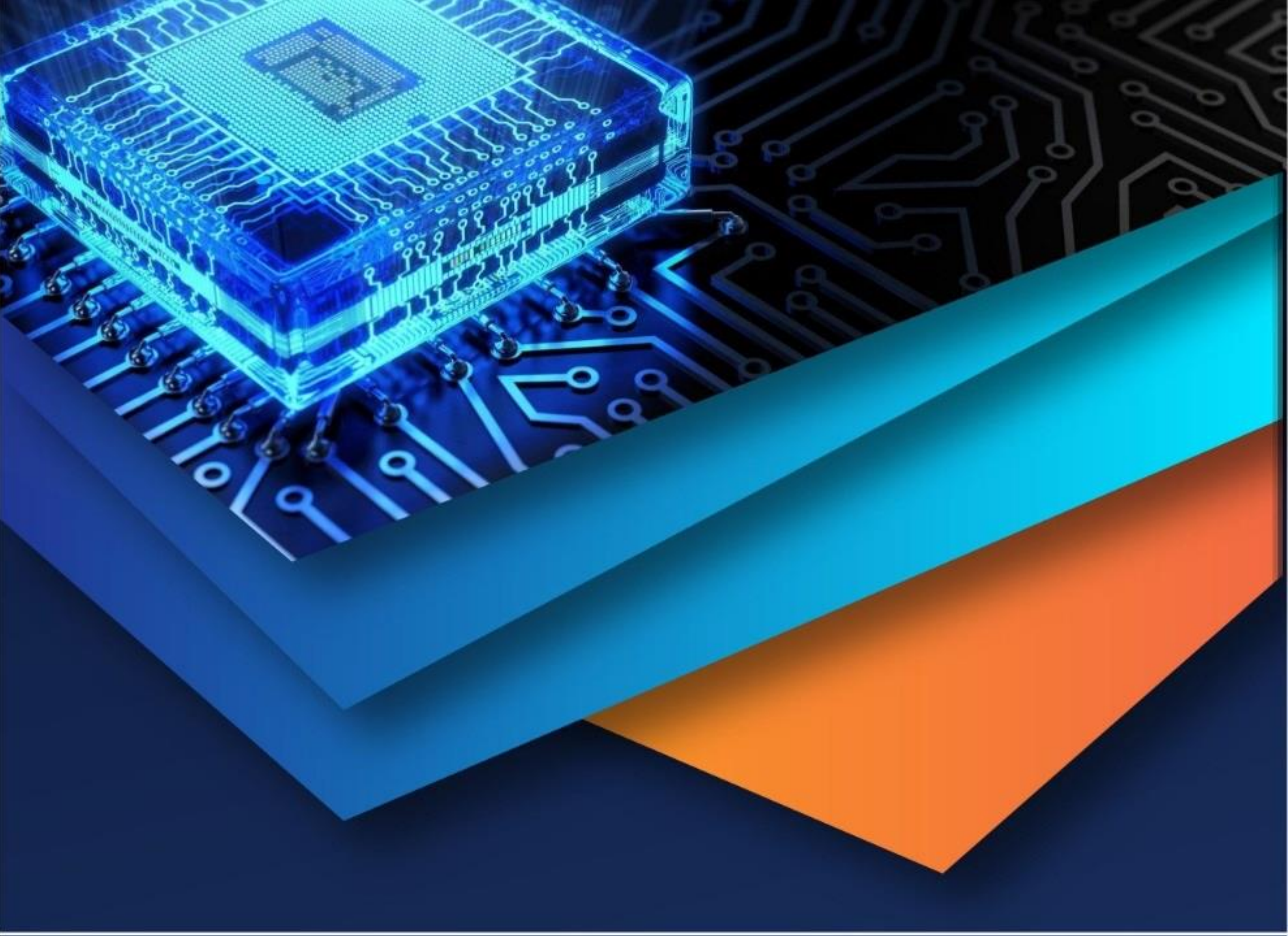

10.22214/IJRASET

INDEX COPERNICUS
45.98

IMPACT FACTOR:
7.129

TOGETHER WE REACH THE GOAL
IMPACT FACTOR:
7.429

INTERNATIONAL JOURNAL FOR RESEARCH

IN APPLIED SCIENCE & ENGINEERING TECHNOLOGY